BRDF correction of S3 OLCI water reflectance products

Davide D'Alimonte[1], Tamito Kajiyama[1], Marco Talone[2], Jaime Pitarch[3], Vittorio Brando[3], Constant Mazeran[4], Michael Twardowski[5], Srinivas Kolluru[5], Alberto Tonizzo[6], Ewa Kwiatkowska[7], David Dessailly[7] and Juan Ignacio Gossn[7]
(1) AEQUORA, Lisboa, Portugal (2) ICM, Barcelona, Spain (3) CNR ISMAR, Roma, Italy (4) SOLVO, Antibes, France
(5) FAU, Florida, USA (6) AWF Consulting, Florida, USA (7) EUMETSAT, Darmstadt, Germany

OCEAN OPTICS XXV
OCTOBER 2–7, 2022 | QUY NHON, BINH DINH, VIETNAM

1. Rationale

- ✓ **Ongoing study** to minimize the effects of the Bidirectional Reflectance Distribution Function (BRDF) and deliver Sentine3 OLCI fully normalized water reflectances.
- ✓ **BRDF correction step-by-step**:
  - Retrieve IOPs from the water reflectances.

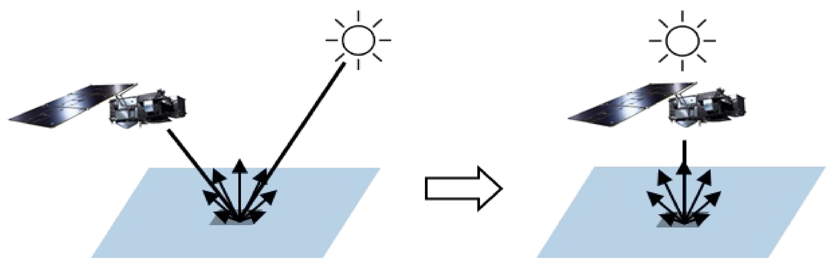

  - Compute water reflectances based on RTE and the given IOPs. One RTE solution corresponds to the actual measurement case and the other to the case with the sun at zenith and the sensor looking towards nadir. Their ratio is the BRDF-correction coefficient.
- ✓ Former steps are the basis of the BRDF correction schemes considered in this study:
  - Morel et al. (2002) → **M02**
  - Park and Ruddick (2005) → **P05**
  - Lee et al. (2011) → **L11**
  - He et al. (2017) → **H17**
  - Twardowski and Tonizzo (2018) → **T18**
- ✓ Differences between these methods depend on how IOPs are retrieved, which approach is adopted to handle the RTE computed solution (with look-up-tables or through an analytical expression), or if an iterative procedure is employed to recompute IOPs to enhance the accuracy of BRDF correction results.
- ✓ **Study rationale:** evaluate the BRDF correction performance and select the scheme most suited for the operational OLCI L2 data processing.

2. Strategy

- ✓ **Synergies** with ongoing EUMETSAT studies on atmospheric correction to ensure consistency between the BRDF development and other components of the processing chain.
- ✓ **Open-source** and publicly available BRDF correction code with a modular design to ease updates and independent applications.
- ✓ BRDF-correction module also scoped for integration within the in-situ **HyperInSPACE community processor**.

3. Highlights

- ✓ **In progress:** setup of the BRDF-correction schemes within the OLCI L2 processor.
- ✓ **Started:** select among the considered BRDF correction schemes the one with the best performance for operational use.
- ✓ **Diagnostic data:** include match-ups, as well as OLCI-A and B images collected during the **tandem phase**.
- ✓ **Data product generation and validation:** rely on in-house processing capabilities and dedicated IT resources for operational services such as **Copernicus Marine Sevice**.
- ✓ **Validation:** between actual and corrected reflectances.

4. Simulated data

- ✓ BRDF correction models tested with **simulated Rrs spectra** from both case-1 (left) and case-2 (right) waters.
- ✓ Results, displayed only for a selected subset of IOPs configurations and BRDF models, show **similar trends but also specific features with respect to both Hydrolight and independent Monte Carlo simulations.**

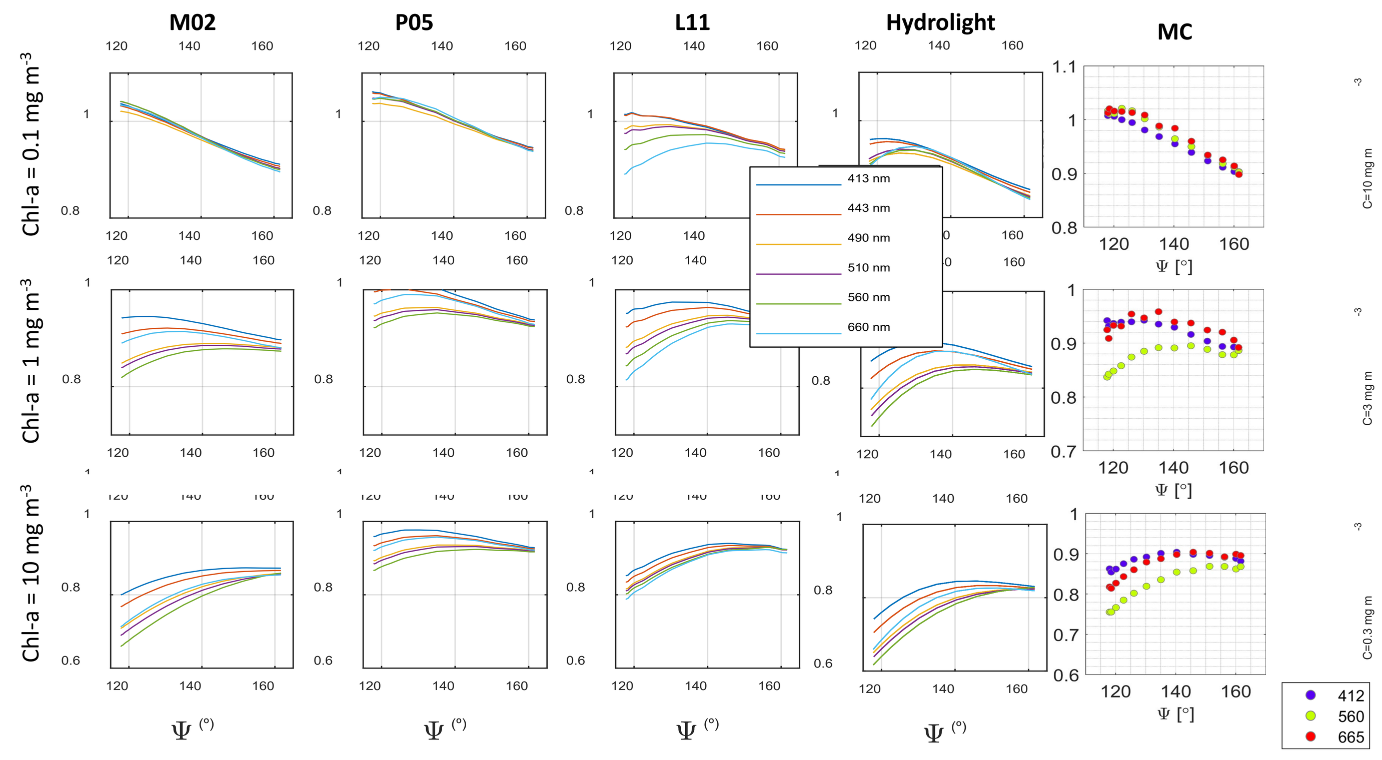

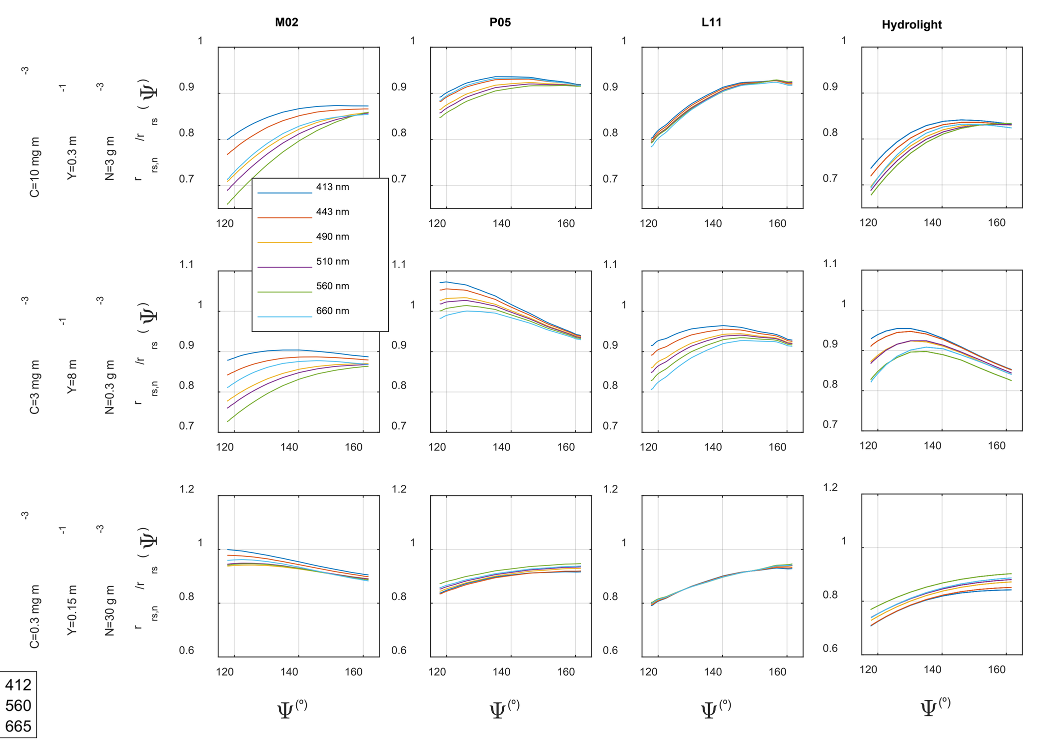

5. In situ data

- ✓ **Assessments** with OFS radiometric data from Black and Med Sea (Talone et al, 2018)

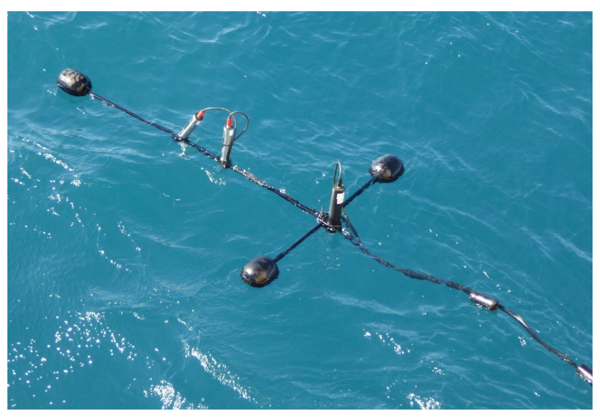

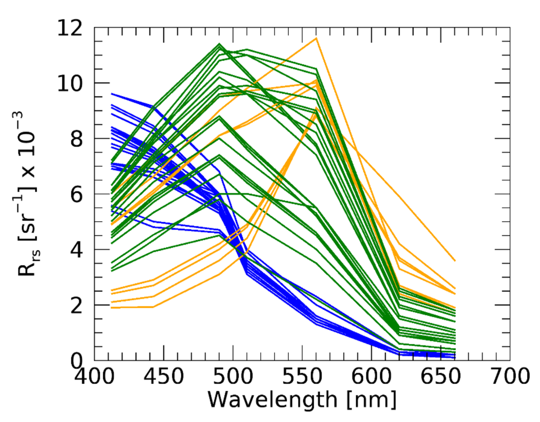

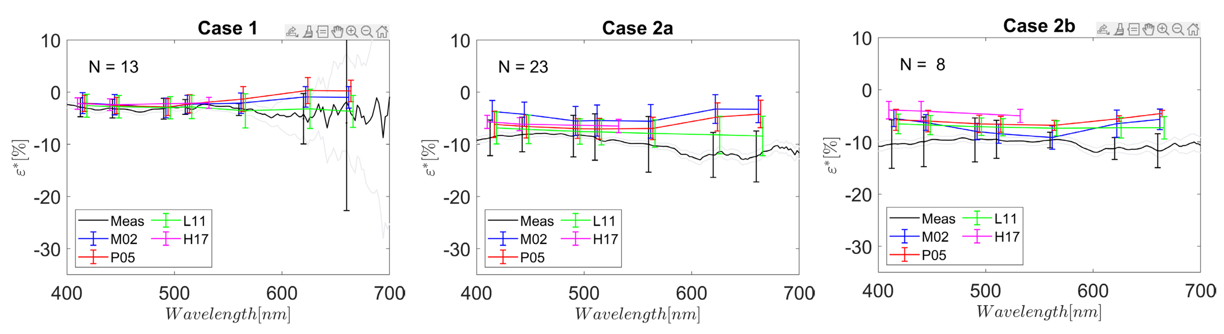

6. Uncertainty

- ✓ **Replicability** relying on the CoastColour dataset (Nechad et al, 2015)

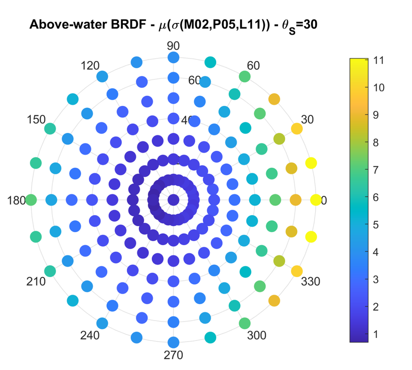

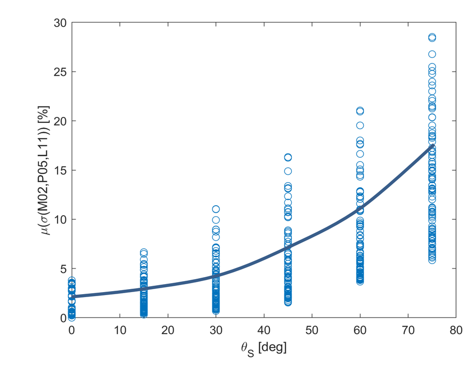

- ✓ **Sensitivity** to uncertainty on IOPs

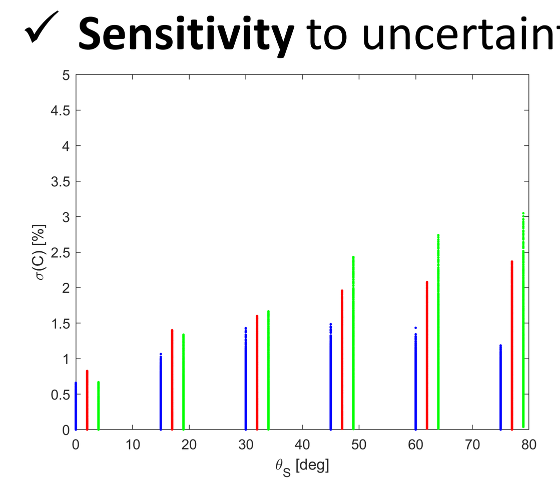

Response of the BRDF correction to a 10% (std) change of the IOPs

7. OLCI data

OLCI image processing.

- ✓ The left and center column panels show uncorrected and corrected (L11) water reflectance maps at 443, 510 and 665 nm from top to bottom rows.
- ✓ The maps in the right column display larger differences in coastal areas.

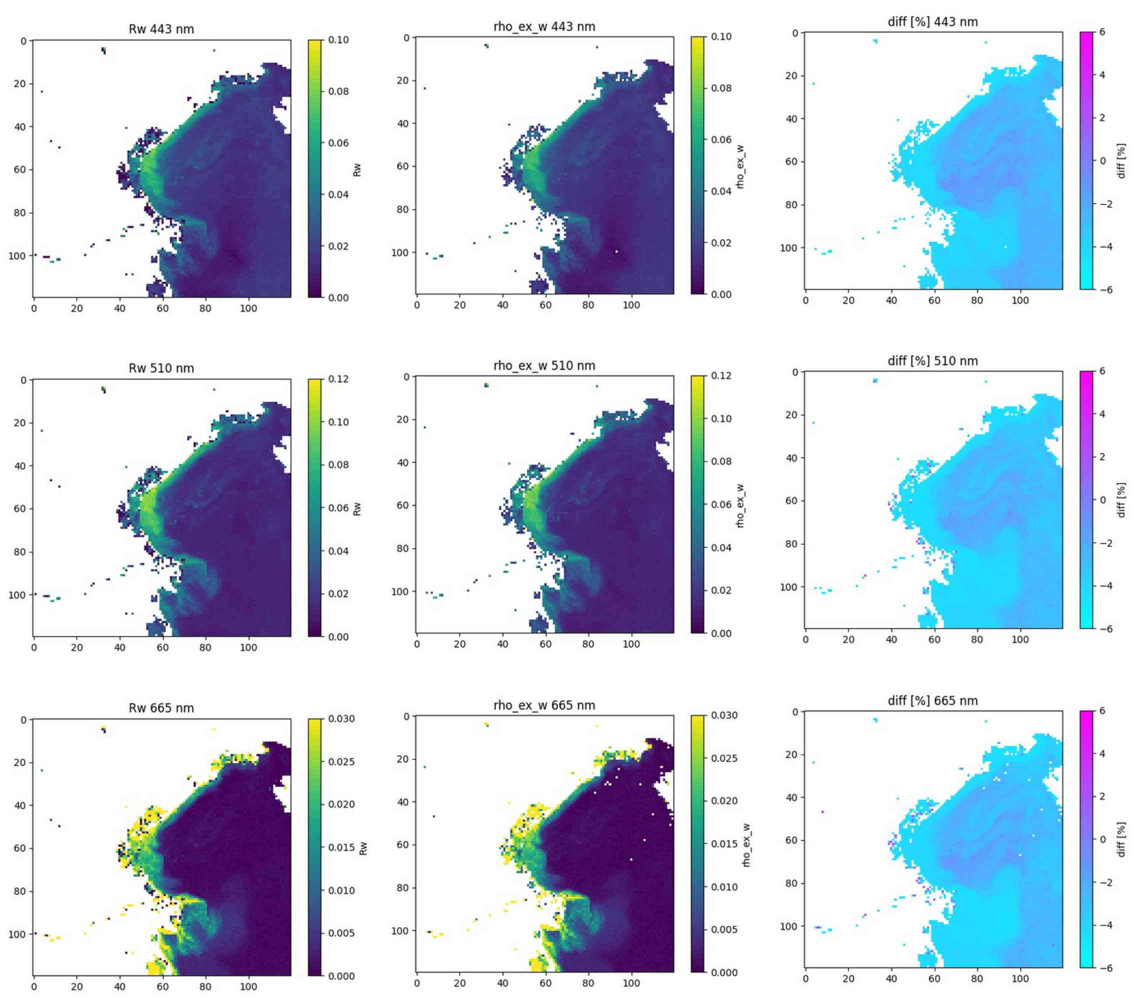

- ✓ BRDF correction at a given point (i. e., Venice AERONET-OC) in view of match-up data analysis.

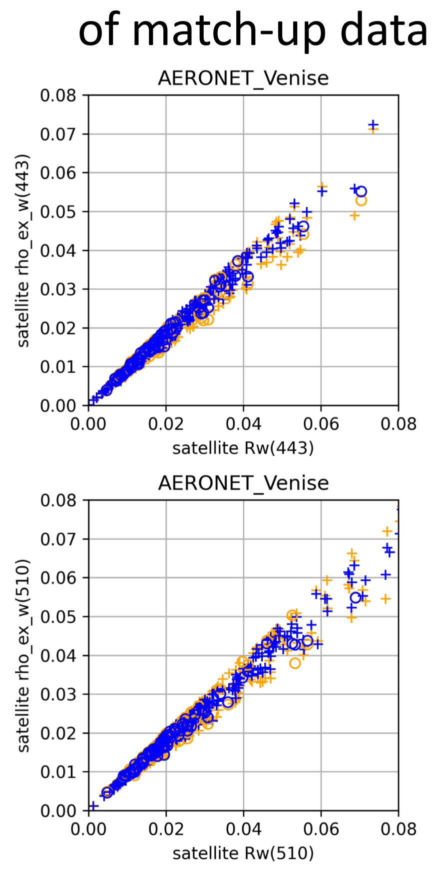

X: satellite non corrected
Y: satellite corrected

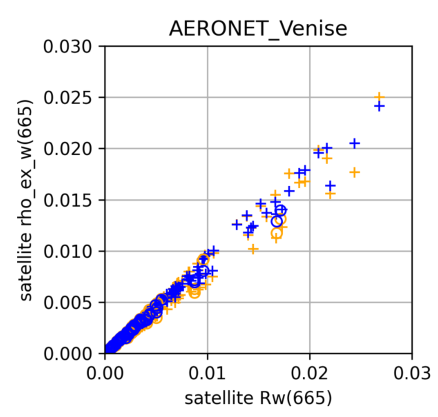

References

1.He, S., 2017, et al., 2017 A Bidirectional Subsurface Remote Sensing Reflectance Model Explicitly Accounting for Particle Backscattering Shapes. J. Geophys. Res. Oceans 122, 8614–8626.
2.Lee, Z.P., et al., 2011. An inherent-optical-property-centered approach to correct the angular effects in water-leaving radiance. Appl. Opt. 50, 3155.
3.Morel, A. et al., 2002. Bidirectional Reflectance of Oceanic Waters: Accounting for Raman Emission and Varying Particle Scattering Phase Function. Appl Opt. 41, 6289–6306.
4.Park, Y.-J., Ruddick, K., 2005. Model of remote-sensing reflectance including bidirectional effects for case 1 and case 2 waters. Appl. Opt. 44, 1236–1249.
5.Talone, M., Zibordi, G., Lee, Z., 2018. Correction for the non-nadir viewing geometry of AERONET-OC above water radiometry data: an estimate of uncertainties. Opt. Express 26, A541.
6.Twardowski, M., Tonizzo, A., 2018. Ocean Color Analytical Model Explicitly Dependent on the Volume Scattering Function. Appl. Sci. 8, 2684
7.Nechad, B. et al, 2015. CoastColour Round Robin datasets, Version 1. PANGAEA, https://doi.org/10.1594/PANGAEA.841950

Acknowledgements EUMETSAT Contract Ref.: RB_EUM-CO-21-4600002626-JIG

Contact

Davide D'Alimonte
AEQUORA
davide.dalimonte@aequora.org

Juan Ignacio Gossn
EUMETSAT
JuanIgnacio.Gossn@eumetsat.int